

Ա.Ի. ԱԼԻԽԱՆՅԱՆԻ ԱՆՎԱՆ ԱԶԳԱՅԻՆ ԳԻՏԱԿԱՆ ԼԱԲՈՐԱՏՈՐԻԱ
(ԵՐԵՎԱՆԻ ՖԻԶԻԿԱՅԻ ԻՆՍՏԻՏՈՒՏ)

ՀԱՅՐԱՊԵՏՅԱՆ ԱՐԱՄ ԱՐՄԵՆԻ

ՍՏԱՆԴԱՐՏ ՄՈԴԵԼԻՑ ԴՈՒՐՍ ԵՐԿԱՐ ԱՊՐՈՂ ՄԱՍՆԻԿՆԵՐԻ ՈՐՈՆՈՒՄԸ CMS (LHC)
ԳԻՏԱՓՈՐՁՈՒՄ ԵՎ ԿՈՐՐԴԻՆԱՏԱՅԻՆ ՈՒ ԺԱՄԱՆԱԿԱՅԻՆ ՄԵԾ ՃՇՏՈՒԹՅԱՆ
ԿԻՍԱՀԱՂՈՐԴՉԱՅԻՆ ԴԵՏԵԿՏՈՐՆԵՐԻ ՄՇԱԿՈՒՄԸ:

Ա.04.16 - «Միջուկի, տարրական մասնիկների և տիեզերական ճառագայթների ֆիզիկա»
մասնագիտությամբ ֆիզիկա-մաթեմատիկական գիտությունների թեկնածուի գիտական
աստիճանի հայցման ատենախոսության

ՍԵՂՄԱԳԻՐ

ԵՐԵՎԱՆ - 2026

A.I. ALIKHANYAN NATIONAL SCIENCE LABORATORY
(YEREVAN PHYSICS INSTITUTE)

HAYRAPETYAN ARAM

SEARCH FOR LONG-LIVED PARTICLES BEYOND THE STANDARD MODEL WITH THE CMS
(LHC) EXPERIMENT AND DEVELOPMENT OF HIGH-PRECISION SPATIAL
AND TIMING SEMICONDUCTOR DETECTORS.

of Dissertation in 01.04.16 – “Nuclear, elementary particle and cosmic ray physics” for the
degree of candidate in physical and mathematical sciences

SYNOPSIS

YEREVAN – 2026

Ատենախոսության թեման հաստատված է Ա.Ի. Ալիխանյանի անվան Ազգային Գիտական
Լաբորատորիայի (ԵրՖԻ) գիտական խորհուրդում:

Գիտական ղեկավար՝

Ֆիզ. մաթ. գիտ. թեկնածու

Արմեն Թումասյան Ռաֆիկի (ԱԱԳԼ)

Պաշտոնական ընդդիմախոսներ՝

Ֆիզ. մաթ. գիտ. դոկտոր

Ալեքսեյ Գուսկով Վյաչեսլավի (ՄՀՄԻ)

Ֆիզ. մաթ. գիտ. դոկտոր

Համլետ Մկրտչյան Գեղամի (ԱԱԳԼ)

Առաջատար կազմակերպություն՝

Երևանի Պետական Համալսարան (ԵՊՀ)

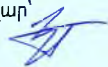
Ատենախոսության պաշտպանությունը կայանալու է 2026 թ. մայիսի 5-ին, ժամը 14:00-ին,
ԱԱԳԼ-ում գործող ԲԿԳԿ-ի 024 «Ֆիզիկայի» մասնագիտական խորհուրդում (Երևան, 0036,
Ալիխանյան Եղբայրների փ. 2):

Ատենախոսությանը կարելի է ծանոթանալ ԱԱԳԼ-ի գրադարանում:

Սեղմագիրն առաքված է 2026 թ. ապրիլի 3-ին:

Մասնագիտական խորհրդի գիտական քարտուղար՝

Ֆիզ. մաթ. գիտ. դոկտոր



Հրաչյա Մարուկյան

The subject of the dissertation is approved by the scientific council of the A.I. Alikhanyan National
Science Laboratory (YerPhI).

Scientific supervisor:

Candidate of ph-math. sciences

Armen Tumasyan (AANL)

Official opponents:

Doctor of ph-math. sciences

Alexei Guskov (JINR)

Doctor of ph-math. sciences

Hamlet Mkrtchyan (AANL)

Leading organization:

Yerevan State University (YSU)

The defense will take place on the 5th of May, at 14:00, during the "Physics" professional council's
session of HESC 024 acting within AANL (2 Alikhanyan Brothers str., 0036, Yerevan).

The dissertation is available at the AANL library.

The synopsis is sent out on the 3rd of April, 2026.

Scientific secretary of the special council:

Doctor of ph-math. sciences



Hrachya Marukyan

General description of the thesis

Importance of obtained results:

1 *Expanding the phase space of the searches for Long-Lived Particles (LLPs) in CMS experiment.*

Particles which have lifetimes which allow them to pass macro-distances before decaying are predicted by many of the Beyond Standard Model theories. Many experiments including the Compact Muon Solenoid (CMS) experiment have done searches of signatures of LLPs with different mass, lifetime, charge etc. CMS detector allows to perform searches of particles in it's subsystems of up to ~ 8 meters from their production point. The searches in more distant subsystems of the CMS detector contribute to the coverage of the phase space of the LLPs with larger lifetimes. In this work the search is performed in the muon system of the CMS detector. LLPs are considered to be produced in B mesons hypothetical decay. The results are provided in terms of upper limit of searched decay depending on model parameters of LLP particles (lifetime and mass). An expanded range of scanned model parameters, along with more stringent limitations, has been achieved compared to earlier results.

2 *Development of an algorithm for the reconstruction of the signals from LLPs.*

LLPs have a different signature in CMS detector than the SM particles. Therefore the development of a reconstruction algorithm for LLPs is necessary, which will be based on the kinematical parameters of the LLP and it's decay remnants. In this work the scenario of LLPs decay into two pions and producing showers in the muon system has been considered.

3 *Testing of the Constant Fraction Discriminator (CFD) Application Specific Integrated Circuit (ASIC).*

CFD is a signal processing method, which allows to perform time-stamping of a signal at a given fraction of it's amplitude. The implementation of this method into a circuit of an ASIC and it's connection to a sensor will allow to find thresholds for signals at a given fraction of the amplitude which will allow to select signals with low amplitudes compared to the fixed threshold method. Also this method will allow to cope with the noisiness of incoming signal and improves the accuracy of the timing measurements.

Investigation of CFD ASIC characteristics in various experimental setups has been performed.

4 *Testing of silicon based AC coupled Low-Gain Avalanche Diodes (LGAD), and development of a testing environment for CMS Endcap Timing Layer (ETL) detector modules.*

The implementation of LGADs into new collider experiments will allow to perform precise time and position measurements. The testing of these devices will contribute to the development of detectors with these sensors as an active medium, by finding the most suitable configurations: thickness, readout method, resistivity and capacitance. LGADs are going to be implemented in a timing detector for CMS, which will be installed in 2026 as a part of the upgrade of CMS for High Luminosity LHC (HL-LHC). A part of this work was the development of a testing environment for the prototypes of this detector cells (modules). This

detector information will allow to disentangle events collected under high luminosity conditions and will have a design timing resolution of several tens of ps ($\sim 30\text{-}50$ ps). Accuracy of the timing measurement is crucial in the attempts assigning detected particles to a specific proton-proton or nucleus-nucleus collision.

Thesis objective:

- *Simulation of the hypothetical signal process, which suggests the production of LLPs in B-mesons decay, under the 2018 CMS conditions, and development of an analysis strategy based on the signature of the LLP.*
- *Search of LLP with B-Parking dataset acquired by CMS in 2018.*
- *Data collection from a circuit which contains the CFD ASIC and an LGAD by radiating the latter with an infrared laser, Ru^{106} beta source and a proton beam of 120 GeV energy, analysis of the collected data and performance of timing and efficiency measurements.*
- *Data collection from strip and pixel LGADs of different configurations, by radiating the latter with 120 GeV proton beams, analysis of the collected data and performance of timing and efficiency measurements.*
- *Development of a testing environment for the ETL detector modules prototypes, collection of data by radiating the ETL modules with a laser and measurement of the timing resolution of the sensors.*
- *Tests with electron and proton beams of 6 GeV (at DESY, Germany) and 120 GeV (at FNAL/CERN US/Switzerland) energy respectively, and measurement of the timing and efficiency.*

Scientific innovation:

- 1 The search of LLPs in the B-hadrons pair production process in pp-collisions with extension of the range of model parameters and tighter limitations to the searched hypothetical signal.
- 2 Achieving less than 30 ps timing resolution using the CFD ASIC with an LGAD sensor using various methods.
- 3 Investigation of characteristics of ETL detector modules prototypes in tests with laser source, electron and proton beams at different energies.

Personal Contribution:

- 1 **Search for long-lived particles in CMS (LHC) 2018 data with pp-collisions using muon detector showers.**
 - MC Simulation of signal process with different model parameters.
 - Development and optimization of clustering algorithms in DT and CSC systems, investigation of their performance.

- Estimation of systematic uncertainties.
- Development of data derived background model.
- Statistical analysis and estimation of upper limits on the searched decay of $B \rightarrow \Phi + K$ (where Φ is denoted as LLP).

2 The development and testing of the Constant Fraction Discriminator ASIC at Fermilab (FCFD).

- Performance of tests using charge injection into the LGAD, which is connected to an ASIC at different bias voltages.
- Measurement of the timing resolution of the ASIC+LGAD assembly using data taken from charge injection.

3 The survey of LGAD sensors with electron and proton beams.

- Installation of the test beam setup at FermiLab Test Beam Facility (FTBF).
- Data acquisition from the irradiated LGADs at different parameters of the setup at different bias voltages and LGAD configurations (thickness, length and type: pixel/strip).
- Data analysis of the strip sensors with $20 \mu m$ thickness, in particular: measurement of the timing resolution and efficiency.
- Development of a testing environment at FNAL, and testing of the first prototypes and the modifications of the ETL modules via charge injection and laser irradiation in the laboratory.
- Analysis of the collected data and measurement of the timing resolution of the modules.
- Participation in the test beam at DESY, with 6 GeV electron beams.
- Participation in the analysis of the collected data at DESY and in measurement of the timing resolution and efficiency.
- Participation in the test beam at FNAL, with 120 GeV proton beams.
- Participation in the analysis of the collected data at FNAL and in measurement of the timing resolution.

Main points for defense:

- 1 Estimation of upper limit for the hypothetical $B \rightarrow \Phi + K$ decay: the upper limit on the branching ratio of the searched decay within considered range of model parameters (mass and lifetime of LLP) estimated to be 10^{-4} .
- 2 Development LLP reconstruction algorithm based on the signals provided by the CMS muon system.
- 3 Results of measurements of the timing resolution of the FCFD ASIC+LGAD assembly and the development of testing.

- 4 Results of measurements of the timing and spatial resolution of LGAD sensors at different parameters of the setup at different bias voltages and LGAD configurations (thickness, length and type: pixel/strip).
- 5 Results of measurements of ETL modules prototypes characteristics.
- 6 Developments of testing environments for the characterization of LGADs and ETL module prototypes.

Conferences:

The results of the dissertation had been reported:

- *LLP - Search for hadronic LLP decays in the muon system using the B-parking dataset, CMS Exotica Workshop 2023, November 30 2023, Centro Congressi Sapienza, Rome, Italy.*
- *Development and characterization of modules for the CMS Endcap Timing Layer for High-Luminosity LHC, APS April Meeting 2024, April 5 2024, Sacramento & Virtual, United States.*
- *Search for Long-Lived Particles with CMS Experiment at the LHC, CHEP-2025, 29 September - 3 October, 2025, Yerevan, Armenia.*
- *Development of precision timing detectors for collider experiments and searches for di-Higgs boson production with the CMS experiment at the LHC, Annual Review Conference-2025, October 5-10 2025, Dilijan, Armenia.*

Publications:

- *Irene Dutta, ... , A. Hayrapetyan et. al, "Results for pixel and strip centimeter-scale AC-LGAD sensors with a 120 GeV proton beam", Nucl.Instrum.Meth.A 1072 (2025) 170224, DOI: 10.1016/j.nima.2025.170224*
- *Si Xie, ... , A. Hayrapetyan et. al, "Design and performance of the Fermilab Constant Fraction Discriminator ASIC", Nucl.Instrum.Meth.A 1056 (2023), DOI: 10.1016/j.nima.2023.168655*
- *A. Hayrapetyan, "The Reconstruction of Long-Lived Particles in the CMS (LHC) Experiment", J.Contemp.Phys. 59 (2024) 4, 353-358, DOI: 10.1134/S1068337225700148*
- *A. Hayrapetyan et. al (CMS Collaboration), "Search for b-hadron decays to long-lived particles in the CMS endcap muon detectors", Phys.Rev.D 113 (2026) 1, 012009, DOI: 10.1103/7ldn-snzn*

Structure of the dissertation:

The dissertation is 127 pages long and includes introduction to the dissertation and to CMS experiment, 4 chapters, a conclusion, 88 references, 88 figures and 19 tables.

Chapter 1

The Large Hadron Collider (LHC) is the largest and the most powerful particle accelerator in the world. It began to operate on September 10, 2008. LHC has a shape of a circle with a circumference of approximately 27-kilometers, which consists of superconducting magnets and accelerating systems. LHC is located in a 50-175 deep underground tunnel, on the border of France and Switzerland. The first collisions were recorded in 2010, in collisions of proton beams of energy of 3.5 TeV. The designed maximum energy of proton-proton collisions at LHC is 14 TeV and instantaneous luminosity $\sim 2 \cdot 10^{34}$ is already achieved. The frequency of the bunch-bunch collisions is 25 ns^{-1} and during each collision up-to 70 particle interactions occur.

LHC stopped operating in 2018 for the purpose of an upgrade and resumed its operation in July 2022. Particles acceleration goes through several stages within various facilities of the CERN accelerator complex. The protons are produced from the ionization of the atoms of Hydrogen and directed to the Linear Accelerator (LINAC, 160 MeV). Afterwards they are directed to the Proton Synchrotron Booster (PSB, 2 GeV), then to the Proton Synchrotron (PS, 16 GeV) and to the Super Proton Synchrotron (SPS, 450 GeV), only then the particle beams are directed into the LHC (13.6 TeV). All of the control systems and technical infrastructure are located at CERN's control center. The particle bunches are colliding in 4 locations along LHC: inside A Toroidal LHC Apparatus (ATLAS), Compact Muon Solenoid (CMS), A Large Ion Collider Experiment (ALICE) and Large Hadron Collider beauty (LHCb) detectors.

CMS (fig.1) is a general-purpose detector at the LHC, designed to perform precise measurements in a wide range of particles energies, up to several TeV. CMS has a broad physics program that includes precise measurements of known and predicted components of the Standard Model, as well as searches for new phenomena beyond it. It has a similar mission to the ATLAS detector, but has different technical solutions and design of the magnetic system. The CMS detector is built on a large solenoid magnet which has a mass of 12.500 tons. The magnet is a coil of superconducting wires that creates 3.8 T magnetic field. The field is confined by a steel yoke. The CMS detector consists of the following subsystems: the tracker system, the electromagnetic (ECAL) and hadron (HCAL) calorimeter, the solenoid magnet and the muon system (MS). Also two detectors are located towards the beam axis at large pseudorapidities: Centauro And Strange Object Research (CASTOR) and Zero Degree Calorimeter (ZDC).

The current data acquisition period will conclude in mid-2026 and will be followed by a long shutdown (Long Shutdown 3, LS3), expected to last nearly four years. During LS3, a major upgrade of the LHC is planned, which will extend its operability by another decade and increase its originally designed luminosity ($1 \cdot 10^{34}$) by a factor of five. The machine configuration is called the high luminosity LHC (HL-LHC). To perform the upgrade challenging technologies have to be developed: 11 to 12 T superconducting magnets; new magnet designs (e.g. canted cosine theta and super-ferric magnet designs), very compact superconducting RF cavities for beam rotation with ultra-precise phase control; new technologies and materials for beam collimation; and high-current superconducting links with almost zero energy dissipation. The peak design luminosity is planned to be $5 \times 10^{34} \text{ cm}^{-2} \text{ s}^{-1}$ and it is planned to collect about $\sim 250 \text{ fb}^{-1}$ per year, with the goal of collecting $\sim 3000 \text{ fb}^{-1}$ in the 12 years after the upgrade. The number of proton-proton

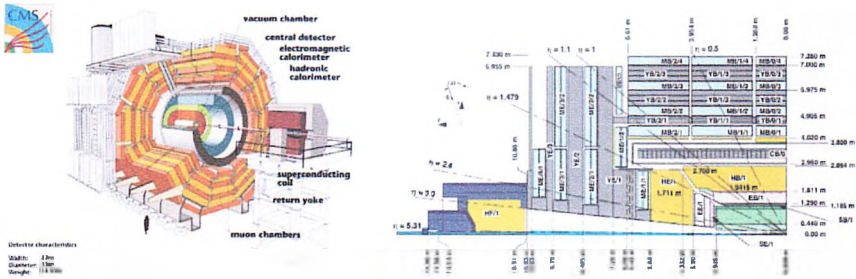


Figure 1: The diagram (left) and the half-longitudinal profile of the CMS detector (right).

interactions per bunch crossing will reach up to around 200. For the preparation of the CMS detector for an efficient operation under HL-LHC regime, a large scale upgrade program will take place during LS3. This will be the most large-scale modernization of CMS since its construction. The following upgrades are intended to be performed: an upgrade of the tracker system, the installation of a high granularity calorimeter, an installation of a MIP timing detector (MTD) layer, upgrade of the muon system and the upgrade of the trigger system of CMS. CMS will be equipped via a new highly granular and 10 times more radiation tolerant tracker system. The outer tracker will be connected to the level-1 trigger system to contribute to the mitigation of the pileup (PU) level. Under high PU regime the reconstruction of the interaction vertices using the 3D tracker information cannot be performed since the interaction vertices overlay. The MTD will provide timing information of the registered particles (4D tracking, fig.2), which can be used to disentangle the overlapping PU. The design timing resolution of the MTD is 30-50 ps. MTD will consist

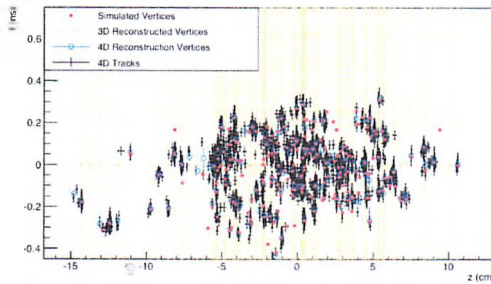


Figure 2: A simulation of the PU interaction vertices vs the interaction time.

of the barrel timing layer (BTL) and endcap timing layer (ETL). For the upgrades in calorimetry, the front-end electronics for ECAL barrel region will be replaced in order to get 30 ps of timing resolution for photons and electrons with energies of 30 GeV at 40 MHz. The avalanche photo-

diodes will be cooled to 9°C which will slow down the aging of the latter. The endcap region of the ECAL and HCAL will be combined into a high granularity calorimeter (HGAL). HGAL will consist of silicon and scintillator detector layers, and interleaved absorbent layers of Pb and CuW in the ECAL region and steel and Cu in the HCAL region of HGAL. The Drift Tube (DT), Cathode Strip Chamber (CSC), and Resistive Plate Chamber (RPC) detectors will be enhanced with upgraded electronics to cope with the 10 times higher particle detection rates and to improve their performance. The upgrade implies installation of new detectors: Gas Electron Multiplier (GEM) chambers. On each endcap of the muon system 2 rings of these detectors will be installed, one of which (GE1/1) has been installed during LS2. The second chamber ring (GE2/1) will be installed during one of the Run 3 end-of-year technical stops. These new detectors will allow amplification of electron charge from 20-25 times. In order to achieve optimal flexibility, the L1-trigger will be based on three independent data processing paths: tracking, calorimetry and the muon system. The HLT will leverage advances in computing, including: massive parallelization using GPUs and heterogeneous computing platforms, machine learning techniques to accelerate and enhance event selection, flexible software framework to handle diverse physics signatures. The HLT will also process larger event sizes due to the inclusion of tracking at L1 and higher detector granularity.

Chapter 2

In this chapter the search for hypothetical long-lived particles (LLPs) in CMS is described. In this dissertation the "Higgs Portal" theoretical model has been probed, which implies addition of a single BSM particle (scalar, pseudoscalar, vector or a neutrino) to the SM. Particularly the addition of a neutral scalar LLP is discussed. The LLP is produced from the decay of a b-quark into an s-quark described in fig.3 (right) diagram. Therefore the search for this process is performed in decays of b-hadrons of 2018 Run 2 experimental data. Several simulated samples are produced to model the $B \rightarrow K + \Phi$ process. where one of B mesons decay via muon production channel ($B \rightarrow \mu\nu_\mu X$) and the other one with LLP and Kaon production (fig.3, left). The muon in first place is used for the event triggering with HLT. The samples are generated inclusively, containing

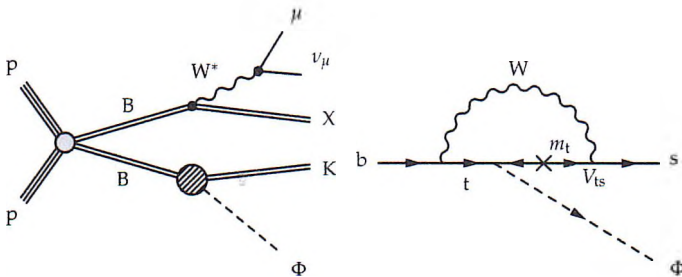


Figure 3: Scheme of the production of a pair of B mesons, where one B meson decays to a muon, neutrino, and another hadron labeled X, while the other B meson decays to a kaon and a LLP Φ (left). Penguin diagram displaying the flavor-changing interaction that produces Φ (right) [1].

decays of B^+ , B^- , and neutral B mesons, in proportion to cross sections derived independently from the B parking data. The search has been done for LLPs with the following masses and proper decay length ($c \times \tau$ where c is the speed of light and τ is the lifetime of the particle in its rest frame): 0.3 GeV and 300, 1000 mm, 0.5 GeV and 500, 5000 mm, 1.0 GeV and 1000, 10000 mm, 2.0 GeV and 2000, 10000 mm and 3.0 GeV and 3000, 10000 mm. These parameters had been used as inputs for simulations. The LLP is expected to decay to a pair of pions ($\Phi \rightarrow \pi^0\pi^0$ or $\Phi \rightarrow \pi^+\pi^-$). The search has been performed in the Muon System (MS) of the CMS detector (the decays beyond the MS region are not considered). To perform the reconstruction of the signal from the LLP decay a clustering algorithm has been used on the recorded hit positions in the MS. The decay of the LLP produces high multiplicity, and spatially compact clusters. The data has been split into two categories: events with clusters in the barrel Drift Tubes (DT) or in endcap Cathode Strip Chambers (CSC). The reconstruction efficiency has been estimated for both categories for different generator parameters: up to 50% in DT and up to 60% in CSC. Selection criteria on the trigger muon and on the cluster parameters had been applied. In both categories the clusters with high multiplicity (greater than 50 hits) which don't match with the trigger muon had been selected. Also the clusters which had been produced in the first layers of both systems had been rejected (since the first layer of the chambers doesn't have any shielding and hadronic jets can also produce high multiplicity clusters). Also the clusters produced in pseudorapidity region of $|\eta| > 1.9$ are rejected since the muon reconstruction efficiency is relatively low in that region. The selected clusters are required to be produced from the main proton-proton interaction and clusters created by the cosmic muons are rejected. In addition different pseudorapidity cuts based on the depth of the cluster and MS stations number are applied as described in details in [1]. In the analysis, background estimation was done with data driven approach using ABCD method. For this method two independent parameters - angular distance between the cluster and trigger muon and the cluster multiplicity had been used. By applying cuts on each of these parameters and selecting a region with higher multiplicity clusters and clusters with larger distance from trigger muons, the signal region (region A) has been selected. Using the number of events in other 3 regions (in which the clusters are considered as produced from background) the background in region A is estimated ($N_A = N_B N_C / N_D$). The signal yield is affected by the uncertainty in the

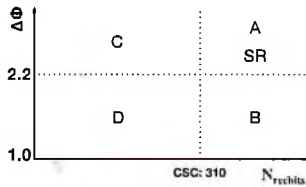


Figure 4: Diagram of the ABCD plane.

integrated luminosity, estimated as 2.5%. When requiring the presence of a muon, a correction factor, referred to as the muon ID scale factor, is applied to account for the differences between the simulated and actual detector response when reconstructing muons. This factor affects the

signal efficiency and its uncertainty is propagated to the signal yield (0.6%). The systematic uncertainty from the limited size of the simulated signal sample is in the range of 13–26%, which is the major source of uncertainty in this analysis. To estimate the systematic uncertainties from potential mismodeling in the simulated signal efficiency of the various cluster-level vetoes, a study was performed using both simulated and recorded samples of $Z \rightarrow \mu^+ \mu^-$ events, where one of the muons underwent bremsstrahlung radiation and produced a cluster in the muon system. The overall systematic uncertainty estimated from the cluster-level vetoes is 9.1%. The total estimated systematic uncertainty is 22–31.5%. To estimate the expected contribution of the jet-induced background the rate at which a jet is misidentified as a signal cluster is measured. The size of the correlated contribution to the total background depends on the proportion of jets that create a shower in the muon system, which is estimated using events enriched in SM jets entering the muon system, provided by a sample of W +jets processes. The background is then subtracted. The upper limit of the BR of the b-hadron to LLP decay process is estimated with a confidence level of 95% as a function of the LLP proper decay length and LLP mass (fig.5). A similar search for LLPs in the muon system, with a different mechanism of LLP production from B decay decay and different LLP decay channels has been performed earlier by CMS collaboration. The signal process from the same theoretical model has been used. In the mentioned previous analysis for different combinations of model parameters (mass, decay distance) of the LLPs $\sim 10^{-3}$ upper limit on BR on $B \rightarrow \Phi$ has been achieved. In this search an improvement has been observed by a factor of 10.

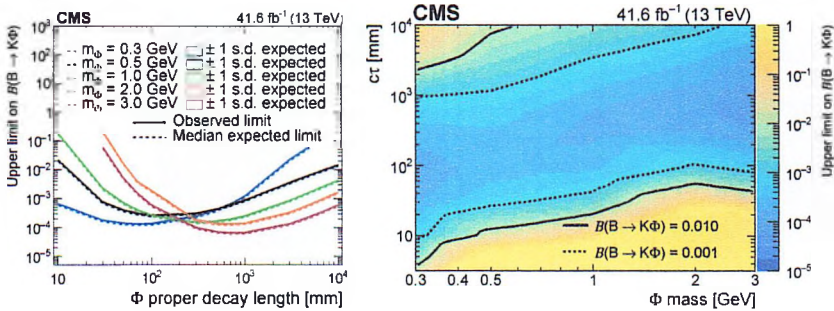


Figure 5: The 95% CL exclusion limits on the $BR(B \rightarrow K\Phi)$, where the scalar LLP, Φ , decays to a pair of pions. Limits are presented for scalar masses $m_\Phi = 0.3, 1.0, 2.0,$ and 3.0 GeV as a function of the Φ mean proper decay length (left) and as a function of LLP mass and proper decay length (right) [1].

Chapter 3

The third chapter is dedicated to the testing of an ASIC, operation of which is based on Constant Fraction Discrimination technique. The ASIC has been produced by TSMC (Taiwan Semiconductor Manufacturing Company) using 65 nm wafers with CMOS (Complementary Metal-

Oxide-Semiconductor) technology. The application of the CFD method will provide the following benefits:

- **higher sensitivity to signals with low amplitudes:** the applied threshold will be a fraction of the maximum amplitude size of the signal (too low amplitude signals can be rejected by a fixed threshold),
- **improved timing measurement accuracy:** the correction of the time-walk effect (dependency of the time of arrival from the signal's amplitude) will not be necessary.

The first prototype of this ASIC (FCFDv0) contains an electrical scheme which processes the incoming electrical signal using the CFD technique. The processing includes the following steps: the input signal is split into two identical copies, one copy is scaled by a constant fraction, the second copy is delayed by a fixed time and the delayed signal is subtracted from the scaled signal forming a bipolar waveform. The timestamp of the signal is defined at the zero-crossing of the bipolar waveform. The first prototype has been tested using charge injection (application of short lasting voltage on the substrate to simulate an interaction with a particle), illumination with a picosecond fast laser with a wavelength of 1062 nm, beta radiation with Ru^{106} source, and 120 GeV proton beam. The CFD ASIC is attached to an AC-coupled Low-Gain Avalanche Diode (AC-LGAD) (fig.6 upper left), the FCFDv0+LGAD assembly is attached to a PCB which is attached to a cooling block, this setup is placed between a radiation source and a Multi-Channel Photomultiplier (MCP-PMT) which acts as a timing reference (fig.6 upper right) due to its high accuracy in timing measurement (~ 10 ps). The testing using the radiation with a proton beam has been

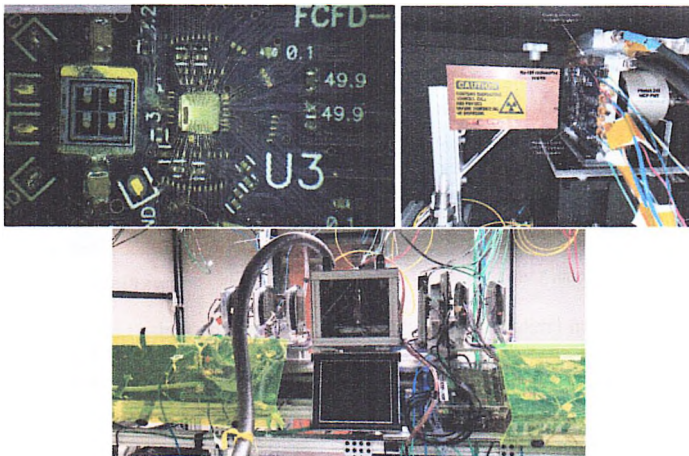


Figure 6: The pictures of the LGAD+FCFDv0 (upper left), the setup for tests with a radiation source (upper right) and the test beam setup (bottom) [2].

performed at FNAL Test Beam Facility (FTBF), which consisted of a tracker system, an MCP-PMT,

a scintillator detector which has been acting as a trigger and the CFD assembly (fig.6 bottom). During all tests a cooling system and a Lecroy Waverunner 8208HD high definition oscilloscope has been used. During the tests using charge injection and laser illumination the Time of Arrival (TOA) of the recorded signals is measured. As timing resolution, the standard deviation of the measured TOA distribution is taken. For the tests with a Ru^{106} beta source and a proton beam the time difference between the TOA and reference time has been calculated and the standard deviation of it's distribution has been taken as timing resolution. In fig.7 the dependency of the timing resolution as a function of injected/deposited charge for charge injection and laser radiation tests, and as a function of bias voltage in case of radiation with beta source and proton beams is presented. During these measurements the resolution of the MCP-PMT has been subtracted in quadrature from the measured resolution. It was possible to achieve ~ 8 ps timing resolution with the charge injection technique at 26 fC injected charge. With the laser measurements it was possible to achieve ~ 11 ps timing resolution at highest applied intensity of the laser, at the accumulated charge of ~ 30 fC. In case of irradiation with the beta source and proton beam the difference between the signal timestamps in LGAD and MCP-PMT is calculated and the resolution of it's distribution is estimated. It was possible to achieve ~ 35 ps timing resolution during both tests at 225 and 200 V bias voltage respectively.

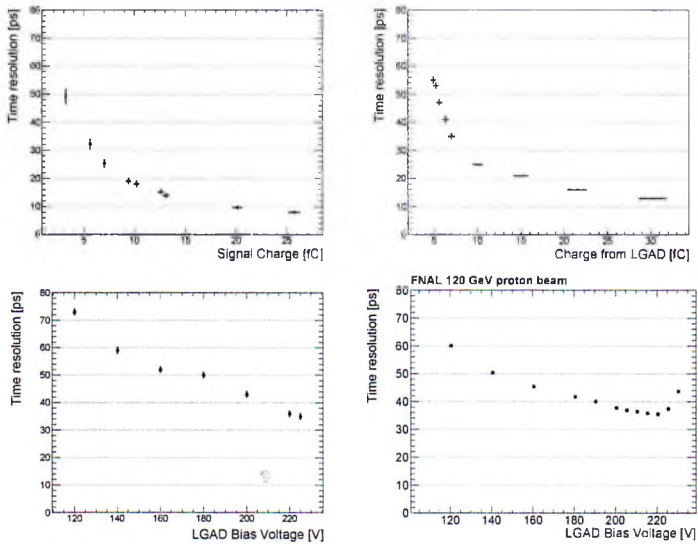


Figure 7: The timing resolution of the LGAD+FCFDv0 vs injected/deposited charge during charge injection (top left) and laser tests (top right), and the timing resolution of the LGAD+FCFDv0 applied bias voltage on AC-LGAD during Ru^{106} beta source (bottom left) and 120 GeV proton beam tests (bottom right) [2].

Chapter 4

The first part of the fourth chapter is dedicated to the survey of AC-coupled LGAD sensors. AC-LGADs are the newer generation types of LGADs which compared to DC-LGADs allow to perform particle registrations across the entire surface of the sensor. This architecture utilizes a capacitive coupling (by implementing an insulator layer between the readout and n+ layer) and a resistive readout of charge from the sensor. In this work pixel and strip AC-LGADs of different thickness (20, 30, 50 μm) and length (0.5, 1 cm) had been tested (fig.8). The pixel samples

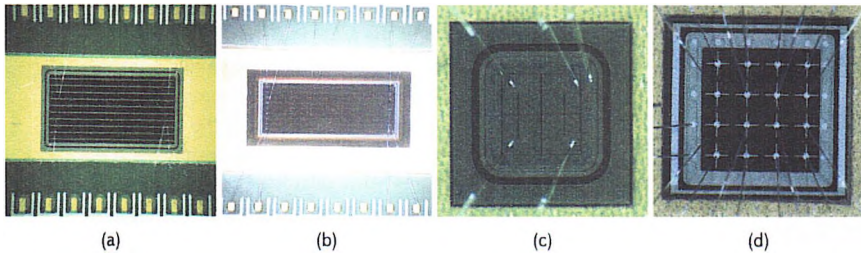


Figure 8: Examples of tested AC-LGAD devices produced by HPK and BNL [3].

had different pixel shape (square, square with rounded corners and cross shaped) and structure (2x2, 4x4), and strip samples had different widths of strip electrodes. These sensors had been produced by Hamamatsu Photonics (HPK) and Brookhaven National Laboratory (BNL). The survey has been performed with a 120 GeV proton beam. In fig.9 the structure of the test beam setup is presented, which consists of a tracker system (which in turn consists of strip and pixel layers) a scintillator which acts as a trigger for the system, an MCP-PMT which acts as a time reference and the tested sensor which is attached to a readout PCB (which in turn is attached to a cooling block). An ethylene glycol-water mix solution was circulated through the block to maintain a uniform and constant temperature of 20°C. Each strip or pixel has been connected to an oscilloscope through the readout board. During the tests the timing and spatial resolution as well as the efficiency of the sensors has been measured. The amplitude vs time waveforms provided by the oscilloscope

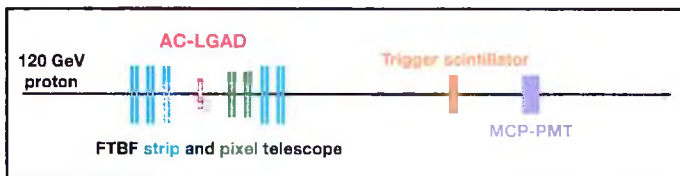


Figure 9: Diagram of the tracking system and the AC-LGAD under test along the beamline [3].

are used to calculate the time of arrival and the corresponding signal amplitude. A reconstruction algorithm has been used to estimate the approximate location of a proton hit based on one/two

adjacent strips or one/several adjacent pixels signals with the highest amplitude. An f value (amplitude fraction) is calculated: $f = \frac{a_1}{(a_1+a_2)}$, where a_1 and a_2 are the two highest amplitude values recorded in the strips. The events should satisfy two conditions: at least two strips must have an amplitude larger than the minimum threshold, amplitude fraction must be less than some value, above which the f no longer varies with the proton impact position and typically occurs close to the metalized strips. The events that fail one of the conditions are considered “one strip” events and the hit position is considered as the center of the leading by amplitude strip. For the events which satisfy the conditions, the found $h(f)$ function is used for each event, and for the f amplitude fraction the corresponding distance relative to the leading strip by amplitude is found and therefore the X position of the hit. In order to reconstruct the Y position of the proton hit the signal propagation time through the strips to the readout electronics is estimated. The acquired data has been analyzed and the efficiency, timing and spatial resolutions had been measured for different AC-LGAD sensors. The relationship between the propagation time for signals in two adjacent strips and the Y position can be done based on the following assumptions: the paths of the signal through the sensor are approximately aligned with the X direction towards the nearest strips, then along the Y direction following the electrode axis, it is assumed that the propagation velocity, v_x (v_y), along the X (Y) directions are approximately the same. The two-channel equivalent reconstruction, for the pixel sensors, is then defined as follows: the leading column contains the metal pad with the largest signal amplitude; the sub-leading column is required to be adjacent to the leading column and should contain a metal pad with the next-largest signal. After the selection of the leading and sub-leading in amplitude pads the same method of the hit position estimation is performed based on the tracker system information. The reconstructed x and y positions are compared to the ones derived from the tracker system to calculate the spatial resolution of the sensor. The spatial resolution of the tracker system ($5 \mu m$) is subtracted in quadrature from the derived resolution. Also the timing resolution has been estimated in different regions of the AC-LGAD surface. The distribution of the difference of the proton arrival time and the time reference (given by the MCP-PMT) is built and the corresponding resolution is estimated. Due to the length of the strip sensors the signal propagation time for different lengths and proton interaction positions will add a time delay to the arrival time. This effect has been considered and a correction has been applied. It was possible to reach ~ 20 , 24 and 35 ps timing resolution respectively for 20 , 30 and $50 \mu m$ thick sensors. The voltages at which the sensors are performing best are close to breakdown voltage. Fig.10 shows the two best-performing pixel sensors from the campaign. The 2×2 HPK pixel sensor with $20 \mu m$ active thickness can achieve a uniform time resolution of ~ 20 ps (fig.10 left). The 4×4 HPK pixel sensor with $20 \mu m$ active thickness can deliver ~ 21 ps timing resolution and 20 - $70 \mu m$ spatial resolution. Spatial resolution values have a reference tracker contribution of $5 \mu m$ subtracted in quadrature.

The second part of the forth chapter is dedicated to the testing and development of module cells of the Endcap Timing Layer (ETL) of the CMS detector, designed for HL-LHC. Two versions of the ETL modules had been tested. Each module consists of 3 main parts: a DC-coupled LGAD sensor, a readout chip for ETL (ETROC) on which the LGAD is attached, and a PCB which is used to transfer information from the ETROC+LGAD system. First module type contains a single ETROC+LGAD system and a PCB design specifically for testing purposes (fig.11, left) and the sec-

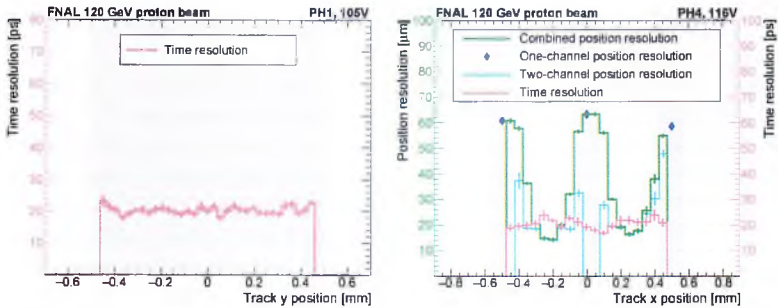


Figure 10: Combines histograms of spatial and timing resolutions for the best performing HPK pixel sensors with 2×2 pads of $500 \mu\text{m}$ metal width with $20 \mu\text{m}$ active thickness (left) and 4×4 pads of $150 \mu\text{m}$ metal width with $20 \mu\text{m}$ active thickness (right) [3].

ond type can contain 4 ETROC+LGAD systems and a PCB which has a closer design to the planned ETL modules (fig.11, right). The ETROC has 16×16 pixel structure, the main components of each pixel of which are: a preamplifier, time to digital converter (TDC), data to analog converter (DAC) and a memory (hit buffer). Each module version has been tested in a laboratory: via charge injection technique and infrared laser irradiation, and radiated via proton and electron beams.

The timing resolution and efficiency had been measured of these two types of modules.

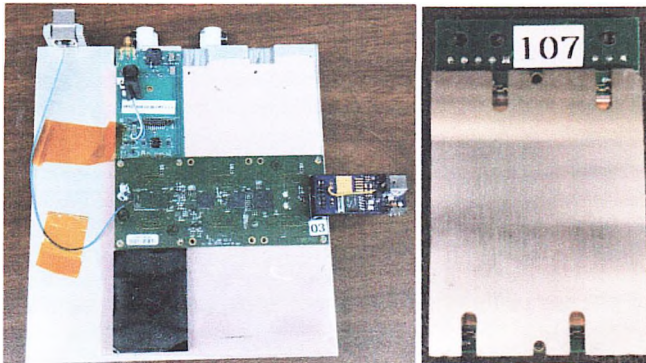


Figure 11: The first prototypes of the testable ETL modules.

Charge injection technique has been periodically used for both versions of modules on the initial stages of their development and during other tests for debugging purposes. The charge injection is repeated for few thousand times for each charge value (4, 6, 8, 10, 12, 15, 20, 25, 30, 32 fC) and the time of arrival (TOA) is measured. The resolution of the TOA distribution is measured and it was possible to achieve 20-40 ps timing resolution for this method for injected 32 fC charge.

The timing resolution measurement has been repeated using an infrared laser setup which

irradiates an attached to ETROC LGAD sensor, and due to the complete deposition of the energy of photons into the LGAD a similar timing accuracy is expected to be measured. In fig.12 the timing resolution as a function of applied threshold on the signal from the injected charge is presented. The distributions of $\Delta T = TOA - (Trigger - Clock)$ for each pixel of the LGAD sensor are presented in fig.13, where "Trigger" refers to the time stamp when the system has been triggered and "Clock" refers to the time stamp of a periodic (40 MHz frequency) signal, which refers to the proton-proton collisions in LHC. It was possible to achieve 25-30 ps across all 4 bonded pixels. It can be seen that the timing resolution is approximately at the same range as derived during charge injection tests. The measurement of the timing resolution and efficiency of the ETROC has been performed using ~ 6 GeV electron beams at DESY. The timing resolution was measured to be ~ 56 ps across different pixels and nearly 100% efficiency has been measured (fig.14, left). The measurements with this module had been repeated at CERN on SPS accelerator with 120 GeV

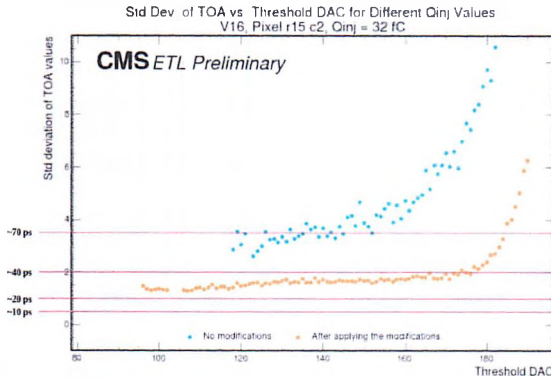


Figure 12: The calculated standard deviation of TOA for different threshold values before and after the modification of module v0 during charge injection with 32 fC charge.

proton beam in April 2024. The resulting measurements showed ~ 20 ps worse timing resolution than in test beam at DESY.

The second version of the modules had undergone series of laboratory tests and modifications. The first test of this module with particle beam has been performed in April 2024 at CERN on SPS accelerator with 120 GeV protons, during which mechanical instability, high electronics noise level, low quality connections between the ETROC and LGAD had been observed. After addressing the mentioned issues the module has been taken to FNAL in June 2024 to perform tests with 120 GeV proton beam. The measured timing resolution of the best performing pixel after the time-walk correction at FNAL has been estimated to be ~ 80 ps. The efficiency of the module has been estimated using the tracker system information of the FNAL test beam stand. The calculated efficiency vs X and Y positions are presented in fig.14. The efficiency of the ETROC has been estimated to be $\sim 40\%$ in average. This version of modules have been tested at CERN SPS synchrotron in October 2024. The testing has been performed for: 19.2, 12.5, 4.0, -4.5, -12.7,

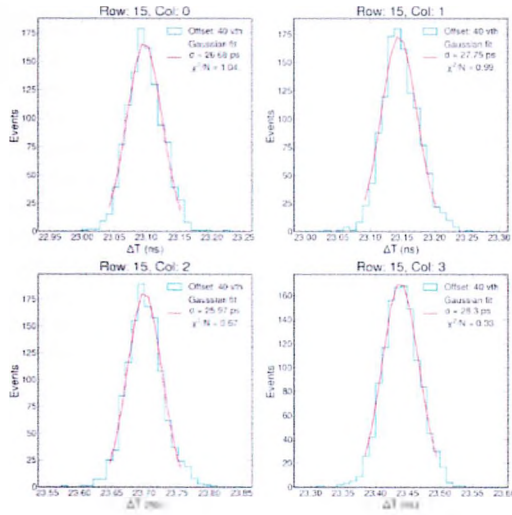


Figure 13: The distribution of ΔT in each pixel of the LGAD.

-20.6 °C. It has been observed that the timing resolution is the best for the lowest temperature and leakage current case. The best timing resolution achieved during this test beam was ~ 56 ps.

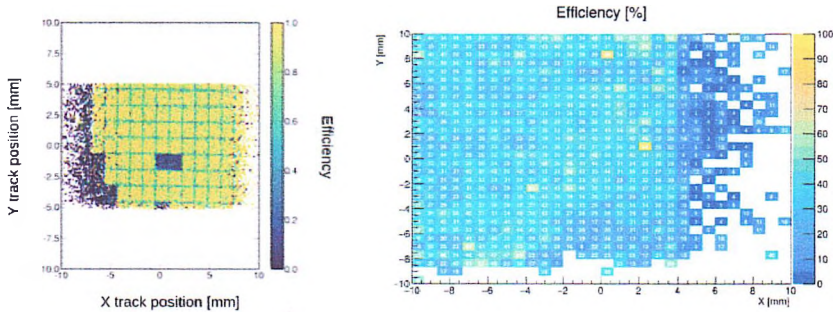


Figure 14: The 2D distribution of the efficiency vs the positions of the reconstructed tracks.

Conclusion

One of the goals of the described search for LLPs, was the expansion of the searches to larger ranges of decay lengths of these particles. This search for LLPs was the second search in the muon system of the CMS detector and the first search with such signature. A clustering algorithm has used and an analysis strategy was developed in order to identify muon detector signals which are generated by the LLPs. The upper limit on the branching ratio of B mesons decay with LLP production was estimated to be 10^{-4} . The estimated upper limits of the branching fraction was compared to the results from a search done earlier in the muon system of CMS, and an improvement by a factor of 10 was observed.

A semiconductor chip based on the Constant Fraction Discrimination (CFD) signal processing technique was tested. The purpose of the CFD chip is to improve the accuracy of particle timing. A detector based on low-gain avalanche diodes (LGADs) attached to CFD ASIC was tested using laser, beta source and proton beam radiation. The timing resolution of approximately 10 ps and 35 ps was achieved in these tests.

Pixel and strip LGAD diodes with AC-LGAD signal recording of different thicknesses (20, 30, and 50 μm) were tested. The tests were conducted using 120 GeV proton beams, during which the timing and spatial resolution and efficiency of these diodes were measured in the regions of the diode surface where the electrodes are located. A timing resolution of approximately 20 and 30 ps was achieved for diodes with thicknesses of 20 and 50 μm , respectively, as well as a spatial resolution of 20-30 μm .

Testing and development of module cells of the Endcap Timing Layer (ETL) of the CMS detector designed for HL-LHC was performed. Testing work was completed on two prototype pixel (16x16 pixel) semiconductor detectors. Measurements were conducted using laser, proton, and electron beams with energies of 120 and 6 GeV, respectively, during which the timing resolution and efficiency of the prototypes were measured. During testing of the first prototype, a timing resolution of approximately 25 and 55 ps was achieved using laser and electron beams, respectively. The efficiency with electron beams was estimated to be approximately 100%. Testing of the second prototype achieved approximately 80 ps of time resolution using proton beams at FNAL and CERN, and achieved approximately 40% efficiency.

Publication list

1. **Aram Hayrapetyan** et. al (CMS Collaboration), "Search for b-hadron decays to long-lived particles in the CMS endcap muon detectors", *Phys. Rev. D* 113 (1 Jan. 2026), p. 012009. DOI: 10.1103/7ldn-snzn.
2. Si Xie, Artur Apresyan, Ryan Heller, Christopher Madrid, Irene Dutta, **Aram Hayrapetyan**, Sergey Los, Cristián Peña, Tom Zimmerman, "Design and performance of the Fermilab Constant Fraction Discriminator ASIC", *Nuclear Instruments and Methods in Physics Research Section A: Accelerators, Spectrometers, Detectors and Associated Equipment* 1056 (2023), p. 168655. ISSN: 0168-9002. DOI: <https://doi.org/10.1016/j.nima.2023.168655>.
3. Irene Dutta, Christopher Madrid, Ryan Heller, Shirsendu Nanda, Danush Shekar, Claudio San Martín, Matías Barría, Artur Apresyan, Zhenyu Ye, William K. Brooks, Wei Chen, Gabriele D'Amen, Gabriele Giacomini, Alessandro Tricoli, **Aram Hayrapetyan**, Hakseong Lee, Ohannes Kamber Köseyan, Sergey Los, Koji Nakamura, Sayuka Kita, Tomoka Imamura, Cristian Peña, Si Xie, "Results for pixel and strip centimeter-scale AC-LGAD sensors with a 120 GeV proton beam", *Nuclear Instruments and Methods in Physics Research Section A: Accelerators, Spectrometers, Detectors and Associated Equipment* 1072 (2025), p. 170224. ISSN: 0168-9002. DOI: <https://doi.org/10.1016/j.nima.2025.170224>.
4. **Aram Hayrapetyan**, "The Reconstruction of Long-Lived Particles in the CMS (LHC) Experiment", *J.Contemp.Phys.* 59.4 (Mar. 2025), p. 6. DOI: 10.1134/S1068337225700148.

Айрапетян Арам

Поиск долгоживущих частиц за пределами Стандартной Модели в эксперименте CMS(LHC) и разработка полупроводниковых детекторов с высокой пространственной и временной точностью

Резюме

Поиском долго-живущих частиц (LLP) в эксперименте CMS была протестирована модель скалярного Хиггсовского портала в данных Run 2 2018 года. Были использованы моделированные данные со следующими параметрами генерации (масса и длина пробега до распада частицы соответственно)-0.3 ГэВ и 300, 1000 мм, 0.5 ГэВ и 500, 5000 мм, 1.0 ГэВ и 1000, 10000 мм, 2.0 ГэВ и 2000, 10000 мм, 3.0 ГэВ и 3000, 10000 мм. Рассматривался гипотетический процесс рождения LLP частиц в распадах В-мезонов, которые в свою очередь распались на пару нейтральных или заряженных пионов в мюонной системе детектора CMS, для реконструкции сигналов которых был разработан алгоритм. Верхний предел BR изучаемого распада ($B \rightarrow K + \Phi$) был оценен в 10^{-4} . Оцененный предел был сопоставлен с результатами похожего поиска проведенного ранее в мюонной системе CMS, в ходе которого было отмечено улучшение чувствительности в 10 раз.

Выполнено тестирование полупроводникового чипа на основе техники обработки сигналов - Constant Fraction Discrimination (CFD). Цель CFD чипа - увеличение точности регистрации времени частиц. Тестировался детектор на основе ливневых диодов с малым коэффициентом усиления (Low-Gain Avalanche Diode, LGAD) при помощи лазерного и радиационного излучения. Было получено около 10-и и 35-и пс временного разрешения в случае с лазерным и радиационным излучением соответственно.

Выполнены работы тестирования пиксельных и стриповых диодов LGAD разных толщин (20, 30, 50 мкм) с регистрацией сигналов переменного тока (AC-LGAD). Тестирования проводились с использованием протонного пучка энергией 120 ГэВ, в ходе которого были измерены временная и пространственная разрешающая способность и эффективность этих диодов в регионах поверхности диода где находятся электроды. Было получено около 20-и и 30-и пс временного а также 20-30 мкм пространственного разрешения для диодов с толщиной 20 и 50 мкм соответственно.

Выполнены работы тестирования 2-х прототипов пиксельных (с конструкцией пикселей 16×16) полупроводниковых детекторов спроектированных для обновления детектора CMS и его оснащения системой регистрации времени частиц в торцевых областях. Тестирования проводились при помощи лазерного излучения, а также протонного и электронного излучений энергией 120 и 6 ГэВ соответственно, в ходе которого были измерены временное разрешение и эффективности прототипов. При тестировании первого прототипа было получено около 25-и и 55-и пс временного разрешения при помощи лазерного излучения, и электронного пучка излучения соответственно, также при помощи электронного излучения эффективность была оценена примерно 100%. При тестировании второго прототипа было получено около 80 пс временного разрешения используя протонное излучение в FNAL и в CERN-е и ~40% эффективность.

Հայրապետյան Արամ

Ստանդարտ մոդելից դուրս երկար ապրող մասնիկների որոնումը CMS (LHC) գիտափորձում և կոորդինատային և ժամանակային մեծ ճշտության կիսահաղորդչային դետեկտորների մշակում

Ամփոփագիր

Իրականացվել է Ստանդարտ մոդելից դուրս երկար ապրող մասնիկների (LLP) որոնումը CMS գիտափորձում օգտագործելով 2018թ-ի փորձարարական տվյալները: Որոնվող հիպոթետիկ մասնիկը կանխատեսվում է Սկայար Հիգգսի պրոտալ մոդելի շրջանակներում և կարող էր առաջանալ, մասնավորապես, B-մեզոնների տրոհումներում: Իրականացվել է հիպոթետիկ ազդանշանի մոդելավորում որոնվող LLP-մասնիկի զանգվածի և կյանքի տևողության (վազքի երկարության) հետևյալ արժեքների դեպքում՝ 0.3 ԳԷՎ և 300, 1000 մմ; 0.5 ԳԷՎ և 500, 5000 մմ; 1.0 ԳԷՎ և 1000, 10000 մմ; 2.0 ԳԷՎ և 2000, 10000 մմ; և 3.0 ԳԷՎ և 3000, 10000 մմ: LLP-մասնիկի որոնումը իրականացվել է CMS-ի մյուոնային համակարգում պիոնային զույգի տրոհման ենթադրյալ կանալով: Մշակվել է այգորիթմ այս մասնիկներից ազդանշանները վերականգնելու համար: Ուսումնասիրված տրոհման հավանականության (BR) վերին սահմանը ($B \rightarrow K + \Phi$) գնահատվել է 10^{-4} : Վերջինս համեմատվել է CMS մյուոնային համակարգում նախկինում կատարված նմանատիպ որոնման արդյունքների հետ, որը ցույց է տվել զգայունության 10-անգամ բարելավում:

Կատարվել է կիսահաղորդչային չիպի փորձարկում՝ հիմնված Constant Fraction Discrimination (CFD) ազդանշանների մշակման մեթոդի վրա: CFD չիպի նպատակն է բարձրացնել մասնիկների գրանցման ժամանակի չափման ճշգրտությունը: Փորձարկվել է ցածր ուժեղացմամբ հեղինդային դիոդների (Low Gain Avalanche Diode, LGAD) վրա հիմնված դետեկտոր՝ օգտագործելով լազերային և էլեկտրոնային/պրոտոնային փնջերով ճառագայթում: Հնարավոր է եղել հասնել ~ 10 և ~ 35 պկվ ժամանակային լուծողականության համապատասխանաբար լազերով և էլեկտրոնային/պրոտոնային ճառագայթման միջոցով:

Կատարվել է տարբեր հաստությունների (20, 30, 50 մկմ) փոփոխական հոսանքի ազդանշանի գրանցումով (AC-LGAD) պիքսելային և ստրիպային LGAD դիոդների փորձարկումը որը իրականացվել է 120 ԳԷՎ էներգիայով պրոտոնային փնջերով ճառագայթման միջոցով, որի ընթացքում չափվել են այդ դիոդների ժամանակային և տարածական լուծողականությունը և էֆեկտիվությունը դիոդի մակերեսի այն հատվածներում, որտեղ գտնվում են էլեկտրոդները: 20 և 50 մկմ հաստությամբ դիոդների համար ստացվել է ~ 20 և ~ 30 պկվ ժամանակային լուծողականություն, ինչպես նաև 20-30 մկմ տարածական լուծողականություն:

Կատարվել է CMS դետեկտորի արդիականացման և վերջինիս եզրային մասի համար նախատեսված ժամանակային դետեկտորների երկու նախատիպային պիքսելային (16×16 պիքսել) կիսահաղորդչային դետեկտորների փորձարկումը լազերային և համապատասխանաբար 120 և 6 ԳԷՎ էներգիաներով պրոտոնային և էլեկտրոնային փնջերի միջոցով, որի ընթացքում չափվել են այդ դետեկտորների ժամանակային լուծողականությունը և էֆեկտիվությունը: Առաջին նախատիպի փորձարկումը տվել է ~ 25 և ~ 55 պկվ ժամանակային լուծողականություն՝ օգտագործելով համապատասխանաբար լազերային և էլեկտրոնային փնջերով ճառագայթում, և $\sim 100\%$ էֆեկտիվություն էլեկտրոնային փնջերով ճառագայթման միջոցով: Երկրորդ նախատիպի փորձարկումը տվել է ~ 80 պկվ լուծողականություն՝ օգտագործելով պրոտոնային փնջեր FNAL-ում և CERN-ում, և $\sim 40\%$ էֆեկտիվություն:

